https://doi.org/10.70750/GEP.2026.3-4.7

FORGÓ ÉS EGYENESVONALÚ HALADÓ MOZGÁST VÉGZŐ TALAJMŰVELŐ SZERSZÁMOK REZGÉSEI: A JELKARAKTERISZTIKA KÜLÖNBSÉGEI ÉS JELFELDOLGOZÁSI KÖVETKEZMÉNYEI

ROTARY VS. LINEAR TILLAGE TOOL VIBRATIONS: DIFFERENCES IN SIGNAL CHARACTER AND IMPLICATIONS FOR SIGNAL PROCESSING

Tamim Deeb[*]*, Dr. László Kátai*[**]

ABSTRACT

Tillage tools move through the soil either by rotation, as in a rotary tiller, or by straight-line traction, as in a cultivator tine. This paper compares the vibrations of the two from the signal processing point of view. Blade entries at fixed rotor angles make the rotary tool's signal periodic in angle, while irregular soil failure makes the linear tool's signal quasi-periodic and largely stochastic. In four recent experimental studies, the motion type rarely guided the choice of processing. A simulation case study then shows that angle-domain methods reveal the blade-pass order and a worn blade of a rotary tiller, whereas the modelled tine wear is best detected by distance-domain features evaluated statistically over windows. The paper closes with recommendations for measurement and processing.

ABSZTRAKT

A talajművelő szerszámok vagy forgó mozgással, mint a talajmaró, vagy egyenes vonalú vontatással, mint a kultivátorkapa, haladnak a talajban. A cikk a kétféle szerszám rezgéseit jelfeldolgozási szempontból hasonlítja össze. A forgó szerszám jele a rögzített rotorszöghelyzetekben bekövetkező késbelépések miatt a szög szerint periodikus, az egyenes vonalú mozgású szerszám jele viszont a talaj szabálytalan törése miatt kváziperiodikus és nagyrészt sztochasztikus. Négy friss kísérleti tanulmány összehasonlítása azt mutatja, hogy a jelfeldolgozási módszer megválasztásakor a mozgás típusát ritkán veszik figyelembe. Egy szimulációs esettanulmány szerint a szögtartománybeli módszerekkel a talajmaró késbelépési rendje és egy kopott kés is kimutatható, a modellezett kapakopás viszont a megtett út szerinti tartományban, szakaszonként statisztikusan kiértékelt jellemzőkkel ismerhető fel a legjobban. A cikk gyakorlati ajánlásokat is megfogalmaz.

1. INTRODUCTION

Soil tillage is one of the most energy-intensive field operations [1], and the condition of the tools affects energy consumption and work quality [2]. Vibration measurement is an attractive way to monitor the tools, since accelerometers can be mounted on the tool or its frame during normal field operation [3, 4].

Tillage tools move through the soil in two different ways. A rotary tiller is driven from the tractor power take-off (PTO), and its blades cut the soil as the rotor turns. A cultivator tine, chisel or subsoiler is drawn through the soil in a straight line. In this paper they are called rotary and linear tillage tools. Both vibrate, but their signals differ in character and call for different processing.

Vibration analysis has its roots in rotating machinery, where a shaft produces a signal that repeats every revolution [5]. The Fourier spectrum, order tracking and time-synchronous averaging exploit this periodicity [6–8]. A rotary tiller inherits it, because each blade enters the soil at a fixed rotor angle [9]. A linear tool has no such reference: its excitation comes from the soil failing irregularly in front of it, so the signal is largely random [10, 11], and its frequency follows the forward speed.

Vibration studies on both tool types exist [3, 4, 11], but their processing is rarely matched to the motion: the periodicity of rotary signals and references such as the rotor angle or the travelled distance may be left unused. A recent review recommends angle-domain processing for agricultural gearboxes and PTO shafts [12], but does not address soil-engaging tools. In our literature search we did not find a systematic comparison of rotary and linear tillage tool vibrations from the signal processing point of view.

To fill this gap, Section 2 contrasts the physical origins of the two signal types, Section 3 compares four recent experimental studies, Section 4 applies identical methods to simulated signals of a rotary tiller with a worn blade and a worn cultivator tine, and Section 5 gives practical recommendations.

** PhD student, Institute of Technology, Hungarian University of Agriculture and Life Sciences (MATE), Páter K. u. 1., H-2100 Gödöllő, Hungary, e-mail: Deeb.Tamim@phd.uni-mate.hu*
*** Full professor, Institute of Technology, Hungarian University of Agriculture and Life Sciences (MATE), Páter K. u. 1., H-2100 Gödöllő, Hungary, e-mail: Katai.Laszlo@uni-mate.hu*

2. ROTARY VS. LINEAR TILLAGE TOOL VIBRATIONS: PHYSICAL ORIGINS AND SIGNAL CHARACTERISTICS

2.1. Rotary tillage tools

The blades of a rotary tiller are staggered on the rotor so that they enter the soil one after another at evenly spaced rotor angles [9]. With rotor speed n (r/min) and Z blade entries per revolution, the blade-pass frequency is

$$f_b = Z \cdot n/60. \quad (1)$$

Each entry produces a cutting-force pulse whose size depends on the bite length, which is set by the ratio of blade tip speed to forward speed [9]; the gearbox adds gear mesh components. Soil heterogeneity changes the size of each pulse but not its timing, which is fixed by the rotor angle. The signal is therefore periodic, more precisely cyclostationary, in angle, like that of a rotating machine [8, 13]. When the PTO speed fluctuates, the harmonics of f_b smear in the spectrum but can be restored by resampling to equal angle increments [6]. A worn blade breaks the symmetry between blades and produces a once-per-revolution modulation, which angle-synchronous averaging can isolate [7].

2.2. Linear tillage tools

A drawn tine pushes a soil block ahead of it until the soil fails along a shear surface; the block breaks away, the force drops, and the cycle repeats [10, 14, 15]. With a typical block length l_f, the soil failure frequency is

$$f_f(t) = v(t)/l_f, \quad (2)$$

where $v(t)$ is the forward speed. Unlike the blade spacing on a rotor, l_f is not a design dimension: it depends on the tool geometry [15], the tine size and the soil moisture [10, 14], and it varies from block to block, so the resulting loads are random [11]. The forward speed also fluctuates with wheel slip. The force excites the tool itself; reported natural frequencies are 5.5–9.4 Hz for a spring-supported sweep [16] and 15–22 Hz for cultivator shanks and tine supports [4, 11]. Stones add isolated impacts. The signal is quasi-periodic at best and largely stochastic.

2.3. Consequences for signal processing

For the rotary tool the natural reference is the rotor angle, derived from the PTO speed. In the angle domain the signal consists of sharp orders, and since every revolution repeats, synchronous averaging suppresses the random soil contribution and reveals blade-to-blade differences.

For the linear tool the natural reference is the travelled distance, available from a radar or GNSS speed sensor. Resampling to distance removes the speed dependence in Eq. (2), but cannot make the signal periodic, because l_f is random. With a coefficient of variation c of the block length, the spectral peak keeps a relative width of the order of

$$\Delta f_f / f_f \sim c \quad (3)$$

even after resampling. As the tine never returns to the same position, synchronous averaging is not applicable; instead, spectra and features are estimated over windows of travelled distance, and changes in tool condition appear as shifts in their distributions. Table 1 summarises the comparison.

Table 1. Rotary and linear tillage tool vibrations compared

Attribute	Rotary tool (rotary tiller)	Linear tool (cultivator tine)
Main excitation	Blade entries at fixed rotor angles	Soil failure cycle, soil variation, stones
Characteristic frequency	$f_b = Z \cdot n/60$ and harmonics	$f_f = v/l_f$, broad, speed-dependent
Signal character	Periodic, cyclostationary	Quasi-periodic to stochastic
Reference signal	Rotor angle (PTO speed)	Distance (radar or GNSS speed)
Suitable processing	Order tracking, angle-synchronous averaging	Distance resampling, windowed spectra and features

3. COMPARISON OF FOUR RECENT CASE STUDIES

Four recent open-access studies with measured data were compared, two on rotary tillers (R1, R2) and two on cultivator tines (L1, L2) (Table 2).

Table 2. Four recent case studies compared

Attribute	R1 [3]	R2 [17]	L1 [4]	L2 [11]
Tool	Rotary tiller, rotor 252 r/min	Walk-behind micro-tiller, cutter roll 2 and 3 r/s	Field cultivator shank	Research cultivator, 12 tines
Sensor	Triaxial accelerometers on tiller gearbox, lower links, axles, cab	Accelerometers on engine, cutter-roll bearing, handle	Accelerometer on shank, GPS-synchronised	Strain gauges on tine supports
Reference signal	None reported	None reported	GPS (georeferencing only)	None reported
Processing	RMS, FFT, PSD, time-frequency	RMS, spectrum, SPH-based model	Vibration with soil moisture, Random Forest, XGBoost	Histograms, autocorrelation, spectrum
Main result	Resonance near 350 Hz with harmonics	Peaks at 3.6 and 7.2 Hz assumed to come from rotor	Soil compaction predicted, $R^2 = 0.87$	Random, weakly autocorrelated loads

Rotary studies. R1 measured a tractor and rotary tiller combination at three forward speeds, with triaxial accelerometers at the tiller gearbox, the lower links, the axles and the cab [3]. RMS values, FFT, power spectral density and time-frequency maps showed a tiller resonance near 350 Hz with harmonics at 700 and 1050 Hz, and vibration rising with speed. No rotor-angle reference or order analysis was reported, although the nominal rotor speed was given. R2 measured a walk-behind micro-tiller at the engine, cutter-roll bearing and handle, and compared RMS values with a model driven by soil forces from smoothed particle hydrodynamics, which matched within 4.3–6.4 % at 3 r/s [17]. At a cutter-roll speed of 2 r/s the bearing showed peaks at 3.6 and 7.2 Hz, which the authors assumed to be related to the rotor. They are not integer multiples of the shaft frequency, and without angle-domain analysis their origin remained unconfirmed.

Linear studies. L1 mounted a GPS-synchronised accelerometer on a cultivator shank and reported the shank's natural frequency (about 21.5 Hz) in the laboratory [4]. Vibration data combined with soil moisture predicted the penetrometer cone index with $R^2 = 0.87$ using Random Forest and XGBoost. GPS served to match vibration to soil samples, not as a processing domain, and no spectral analysis of the field signals was reported. L2 measured the loads on twelve tine supports with strain gauges and treated them explicitly as random vibration [11]. Histograms and autocorrelation showed weakly correlated random signals, and the spectra were compared with the support's natural frequency of 15.15 Hz. The spectra of all twelve supports were nearly identical (correlation ≥ 0.979), suggesting that the excitation is set by the soil and operating conditions rather than by the individual tine.

Synthesis. (i) The linear studies treat the tine signal statistically, in agreement with Section 2.2. (ii) Neither rotary study exploited the periodicity of the rotary tool: blade-pass orders were not separated from resonances, and in R2 the link between peaks and rotor speed was assumed rather than demonstrated. (iii) None of the studies used its natural reference, the rotor angle or the travelled distance, as a processing domain. The motion type is thus rarely used to guide the choice of processing; Section 4 shows with simulated signals what can be lost as a result.

4. SIMULATION CASE STUDY

4.1. Signal models

Acceleration signals of both tool types were synthesised and processed with the same methods. The parameters are plausible assumptions, so the results illustrate Section 2 rather than describe a specific machine.

The rotary tiller is driven from a 540 r/min PTO through a 15/37 bevel gear pair ($n = 218.9$ r/min). With six flanges of four blades, $Z = 24$ and, by Eq. (1), $f_b = 87.6$ Hz. Each blade entry produces an impact and a cutting-force pulse whose amplitude scatters randomly (coefficient of variation 0.25) to represent soil heterogeneity. The forces excite two structural modes, and gear mesh, stones and noise are added. The PTO speed fluctuates by −7/+8 %, and a once-per-revolution tachometer is assumed. In the worn case, blade 1 produces 40 % less force.

The cultivator tine is rigid and works at forward speeds of 2.0, 1.5 and 2.5 m/s with 4 % random speed fluctuation. The force builds up while a soil block is loaded and drops when it fails. The block length is random, with mean $l_f = 75$ mm and $c = 0.25$, so by Eq. (2) f_f ranges from about 19 to 36 Hz. The force excites two tine modes (60 and 420 Hz), and soil strength variation, stones and noise are added. Wear was modelled generically by 20 % longer blocks and 15 % higher force. The travelled distance is the integral of the true (error-free) forward speed.

4.2. Results

The spectrum of the rotary tool consists of sharp lines at f_b, its harmonics and the gear mesh, whereas that of the linear tool shows only broad humps at the tine modes, and its envelope spectrum is spread over the range of f_f (Figure 1).

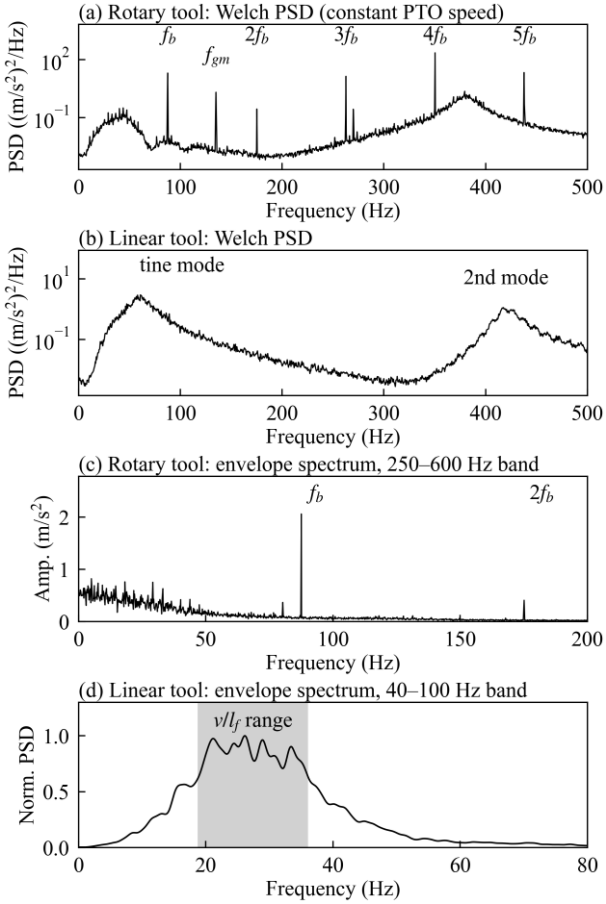

Figure 1. Power spectral density of (a) the rotary and (b) the linear tool; envelope spectra of (c) the rotary and (d) the linear tool (shaded: range of the soil failure frequency)

With fluctuating PTO speed the blade-pass line smears and its peak-to-floor ratio falls from 48.6 to 28.3 dB; angular resampling restores a sharp order 24 at 47.7 dB (Figure 2a, b). Angle-synchronous averaging over 217 revolutions shows the worn blade 3.9 dB below the others, against +0.2 dB for the healthy rotor (Figure 2c, d). In single revolutions the random soil forces mask the fault: the worn blade is the weakest in only 40 % of them.

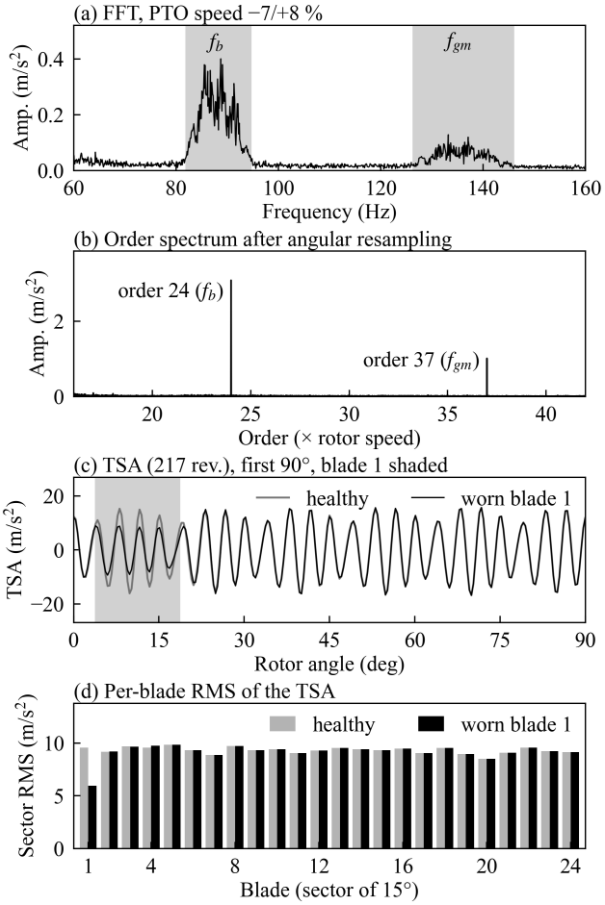

Figure 2. Rotary tool with PTO speed fluctuation: (a) spectrum; (b) order spectrum after angular resampling; (c) angle-synchronous average, healthy and with blade 1 worn; (d) RMS of the average per blade sector

For the linear tool, the soil failure band follows the forward speed (Figure 3a). The time-domain envelope spectrum has a relative width (half-power width over peak frequency) of 0.87. After resampling the envelope to distance, the peak lies at 13.5 1/m, within 1.5 % of $1/l_f$, and the relative width falls to 0.34, but the peak stays broad, of the order of c (Eq. 3; Figure 3b, c). The envelope autocorrelation falls from 0.25 at one block length to nearly zero at ten, while for the rotary tool it remains 0.59 after ten blade spacings, so a distance-synchronous average has nothing to synchronise to.

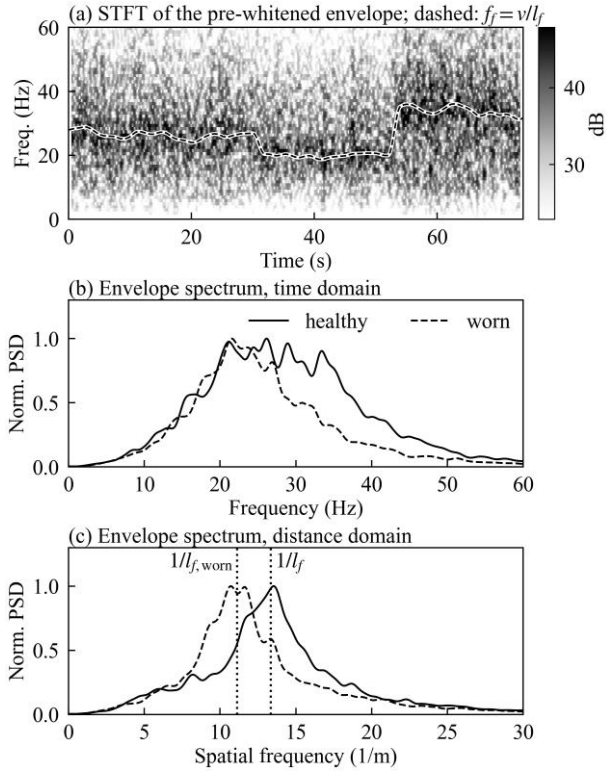

Figure 3. Linear tool: (a) time-frequency map of the envelope, soil failure frequency dashed; envelope spectrum (b) in time and (c) in distance, healthy (solid) and worn (dashed)

The tine condition was therefore assessed over 3 m windows (37 healthy and 35 worn, all stone-free). Of eleven features compared by Cohen's *d* (worn minus healthy mean over pooled SD), the distance-domain ones separated healthy and worn tines best (dominant spatial frequency $d = -1.85$, spatial centroid −1.41; Figure 4). Their time-domain counterparts reached only −0.81 and −0.85 because they follow the speed, and RMS and band energies stayed below 0.5. Stones were isolated transients: an envelope detector found 28 of 29, and the 300–600 Hz kurtosis flagged every window with a stone and none without.

5. SUMMARY

A rotary tiller produces vibration that is periodic in rotor angle, whereas a drawn tine produces quasi-periodic vibration that follows the forward speed and never repeats at a fixed position. The four studies reviewed rarely made use of this difference. In the simulation, angular resampling restored the blade-pass order of the rotary tool from 28 dB to 48 dB above the floor, and angle-synchronous averaging revealed a worn blade 3.9 dB below the others. For the linear tool, distance resampling narrowed the soil failure peak only to the width set by the random block length, synchronous averaging was not applicable, and the modelled tine wear was best detected by distance-domain features evaluated over windows (Cohen's |d| up to 1.85).

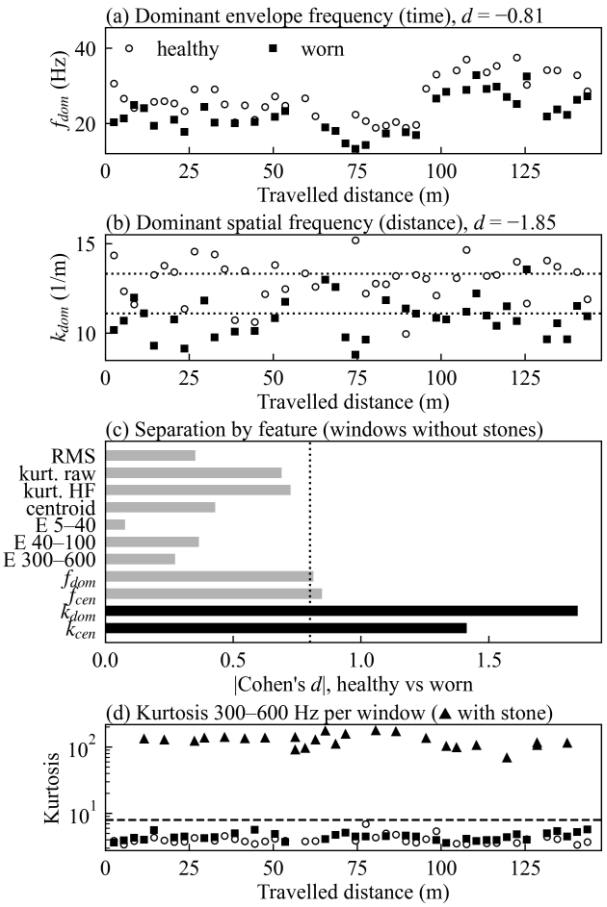

Figure 4. Windowed features of the linear tool: dominant frequency (a) in time and (b) in distance; (c) separation by feature (E: band energy, HF: 300–600 Hz, dom: dominant, cen: centroid; dotted: $|d| = 0.8$); (d) kurtosis per window (triangles: stone; dashed: threshold 8)

The results lead to the following recommendations:

- Record a reference signal with the vibration: the rotor angle or PTO speed for rotary tools, the forward speed from a radar or GNSS sensor for linear tools.
- For rotary tools, resample to the angle domain and use angle-synchronous averaging to compare individual blades.
- For linear tools, resample the envelope to distance and evaluate spectra and features over distance windows; do not expect sharp lines or apply synchronous averaging.
- Judge a change in tool condition from the shift of a feature distribution over many windows, not from a single record.
- Choose the sensor position with the analysis in mind: a shank-mounted sensor also records the shank's own resonance [4], while signals on a bearing housing are strongly influenced by the tractor [18].

As the study used simulated signals with assumed parameters and ideal references, the conclusions should next be verified by field measurements on both tool types. The simulation code is available from the authors on request.

6. REFERENCES

[1] LAL R.: *Carbon emission from farm operations*, Environment International, Vol. 30, No. 7, 2004, pp. 981–990, https://doi.org/10.1016/j.envint.2004.03.005

[2] NATSIS A., PAPADAKIS G., PITSILIS J.: *The Influence of Soil Type, Soil Water and Share Sharpness of a Mouldboard Plough on Energy Consumption, Rate of Work and Tillage Quality*, Journal of Agricultural Engineering Research, Vol. 72, No. 2, 1999, pp. 171–176, https://doi.org/10.1006/jaer.1998.0360

[3] GAO Y., YANG Y., FU S., FENG K., HAN X., HU Y., ZHU Q., WEI X.: *Analysis of Vibration Characteristics of Tractor–Rotary Cultivator Combination Based on Time Domain and Frequency Domain*, Agriculture, Vol. 14, No. 7, 2024, 1139, https://doi.org/10.3390/agriculture14071139

[4] JANBAZIALAMDARI S., FLIPPO D., RIDDER E., BROKESH E.: *Soil Compaction Prediction in Precision Agriculture Using Cultivator Shank Vibration and Soil Moisture Data*, Agriculture, Vol. 15, No. 17, 2025, 1896, https://doi.org/10.3390/agriculture15171896

[5] RANDALL R. B.: *Vibration-based Condition Monitoring: Industrial, Aerospace and Automotive Applications*, Wiley ISBN 978-0-470-74785-8, Chichester, 2011, https://doi.org/10.1002/9780470977668

[6] FYFE K. R., MUNCK E. D. S.: *Analysis of computed order tracking*, Mechanical Systems and Signal Processing, Vol. 11, No. 2, 1997, pp. 187–205, https://doi.org/10.1006/mssp.1996.0056

[7] McFADDEN P. D.: *A revised model for the extraction of periodic waveforms by time domain averaging*, Mechanical Systems and Signal Processing, Vol. 1, No. 1, 1987, pp. 83–95, https://doi.org/10.1016/0888-3270(87)90085-9

[8] ANTONI J., BONNARDOT F., RAAD A., EL BADAOUI M.: *Cyclostationary modelling of rotating machine vibration signals*, Mechanical Systems and Signal Processing, Vol. 18, No. 6, 2004, pp. 1285–1314, https://doi.org/10.1016/S0888-3270(03)00088-8

[9] ZHENG S., LU T., LIU J., TIAN Y., HAN M., TAI M., GAO S., LIU T., WANG D., ZHAO Z.: *Discrete Element-Based Design of a High-Speed Rotary Tiller for Saline-Alkali Land and Verification of Optimal Tillage Parameters*, Agriculture, Vol. 15, No. 3, 2025, 269, https://doi.org/10.3390/agriculture15030269

[10] RAJARAM G.: *Collapse failure in dry clay soils caused by tine implements*, Journal of Terramechanics, Vol. 27, No. 2, 1990, pp. 69–78, https://doi.org/10.1016/0022-4898(90)90001-3

[11] CÂRDEI P., CONSTANTIN N., MURARU V., PERSU C., SFÎRU R., VLĂDUȚ N.-V., UNGUREANU N., MATACHE M., MURARU-IONEL C., CRISTEA O.-D., LAZA E.-A.: *The Random Vibrations of the Active Body of the Cultivators*, Agriculture, Vol. 13, No. 8, 2023, 1565, https://doi.org/10.3390/agriculture13081565

[12] JI K., ZHOU Z., LI Y.: *Vibration-Based Fault Diagnosis of Agricultural Machinery: A Review of Field Excitation, Signal Processing, Intelligent Models and Engineering Deployment*, Machines, Vol. 14, No. 7, 2026, 795, https://doi.org/10.3390/machines14070795

[13] ANTONI J.: *Cyclostationarity by examples*, Mechanical Systems and Signal Processing, Vol. 23, No. 4, 2009, pp. 987–1036, https://doi.org/10.1016/j.ymssp.2008.10.010

[14] RAJARAM G., GEE-CLOUGH D.: *Force-distance behaviour of tine implements*, Journal of Agricultural Engineering Research, Vol. 41, No. 2, 1988, pp. 81–98, https://doi.org/10.1016/0021-8634(88)90191-6

[15] GODWIN R. J.: *A review of the effect of implement geometry on soil failure and implement forces*, Soil and Tillage Research, Vol. 97, No. 2, 2007, pp. 331–340, https://doi.org/10.1016/j.still.2006.06.010

[16] TAMÁS K.: *Modelling the interaction of soil with a passively-vibrating sweep using the discrete element method*, Biosystems Engineering, Vol. 245, 2024, pp. 199–222, https://doi.org/10.1016/j.biosystemseng.2024.06.006

[17] LIU X., HAO W., CHEN Y., HAO Q., ZHANG X., SUN Z.: *Development of Vertical Vibration Model for Micro-Tiller by Smoothed Particle Hydrodynamics Method*, AgriEngineering, Vol. 6, No. 3, 2024, pp. 2481–2493, https://doi.org/10.3390/agriengineering6030145

[18] CECCHINI M., PICCIONI F., FERRI S., COLTRINARI G., BIANCHINI L., COLANTONI A.: *Preliminary Investigation on Systems for the Preventive Diagnosis of Faults on Agricultural Operating Machines*, Sensors, Vol. 21, No. 4, 2021, 1547, https://doi.org/10.3390/s21041547